

Initializing Then Refining: A Simple Graph Attribute Imputation Network

Wenxuan Tu¹, Sihang Zhou¹, Xinwang Liu^{1*}, Yue Liu¹, Zhiping Cai¹, En Zhu¹, Changwang Zhang² and Jieren Cheng³

¹National University of Defense Technology, Changsha, China

²Tencent Technology, Shenzhen, China

³Hainan University, Haikou, China

wenxuantu@163.com, xinwangliu@nudt.edu.cn

Abstract

Representation learning on the attribute-missing graphs, whose connection information is complete while the attribute information of some nodes is missing, is an important yet challenging task. To impute the missing attributes, existing methods isolate the learning processes of attribute and structure information embeddings, and force both resultant representations to *align* with a common indiscriminative normal distribution, leading to inaccurate imputation. To tackle these issues, we propose a novel graph-oriented imputation framework called *initializing then refining (ITR)*, where we first employ the structure information for initial imputation, and then leverage observed attribute and structure information to adaptively refine the imputed latent variables. Specifically, we first adopt the structure embeddings of attribute-missing samples as the embedding initialization, and then refine these initial values by aggregating the reliable and informative embeddings of attribute-observed samples according to the affinity structure. Specially, in our refining process, the affinity structure is adaptively updated through iterations by calculating the sample-wise correlations upon the recomposed embeddings. Extensive experiments on four benchmark datasets verify the superiority of ITR against state-of-the-art methods.

1 Introduction

Graph data, which models the relationships between entities, is ubiquitous in practical scenarios. To handle these data, graph representation learning (GRL) has increasingly become a popular research topic and achieved remarkable success in many real-world applications such as social network analysis [Hu *et al.*, 2017], knowledge graph completion [Wu *et al.*, 2020], etc. It has long been proved that integrating the attribute and structure information while conducting the representation learning is essential for improving the quality of sample embeddings [Kipf and Welling, 2017;

Chen *et al.*, 2022]. However, in most real-world graph applications, only a small portion of samples have complete attribute information. For example, in a co-purchase graph of Amazon, consumers tend to selectively (or entirely not) provide their feedback for specific items due to privacy concerns. Consequently, graph representation learning on incomplete-attribute graphs is becoming an increasingly important task.

Data imputation is a straightforward mechanism to handle incomplete-attribute graphs. Existing efforts combine the imputation-oriented machine learning techniques, e.g., matrix completion [van den Berg *et al.*, 2017; Zhang and Chen, 2020], generative adversarial network [Spinelli *et al.*, 2020], Gaussian mixture model (GMM) [Taguchi *et al.*, 2021], with graph neural networks (GCNs) and propose various attribute-incomplete graph representation learning methods with impressive performance. Although significant progress has been made, the performance of these methods drops drastically when handling attribute-missing graphs, i.e., graphs whose all attribute information of a specific portion of samples is missing. To solve the problem of representation learning on attribute-missing graphs, a recent advanced method named SAT [Chen *et al.*, 2022] introduces a shared-latent space assumption to impute the attribute-missing values at the first attempt. Specifically, SAT first learns the latent representations of attribute and structure spaces independently and then conducts a distribution alignment technique to recover the unknown features of attribute-missing samples. Although SAT achieves encouraging success, when conducting the data imputation, it 1) isolates the learning processes of attribute and structure information embeddings; 2) forces both types of latent variables to align with a common in-discriminative normal distribution. Hence, the negotiation between attribute and structure information tends to get overly rigid, resulting in inaccurate imputation and less discriminative representations.

To overcome the aforementioned issues, this work proposes a novel graph attribute imputation network termed Initializing Then Refining (ITR). To forbid the adverse effect of inaccurate simple initialization and the limitation of rigid assumption, the main idea of our strategy is to make full use of the trustworthy visible information to conduct the sample embeddings for data imputation. As a consequence, on the one hand, we pick out the nodes with complete attributes and learn the sample embeddings by sufficiently combining the attribute and structure information of these samples. On the

*Corresponding author

other hand, we take all the nodes and learn the sample embeddings only according to the structure information. These two processes are illustrated as the upper and underneath pathways in Fig. 1, respectively. The two mentioned operations ensure the quality of latent representations of the nodes with complete attributes, and in the meantime, provide a reasonable initialization to those nodes with missing attributes. After that, to achieve better attribute-missing graph representation learning, the structure embeddings of attribute-missing samples are taken as initial imputed variables and then refined with an adaptively updated affinity structure for embedding refinement. This is illustrated as imputation refinement in Fig. 1. Unlike the prior distribution alignment-based imputation strategy in SAT, our proposed ITR is more general and flexible, since both types of information (i.e., graph structure and node attributes) are allowed to sufficiently negotiate with each other for reliable attribute restoration. The main contributions of this paper are three-fold:

- We propose a simple yet powerful graph attribute imputation network called ITR that can jointly conduct attribute-missing graph representation learning and data imputation without any prior distribution assumption.
- We develop an initializing then refining strategy to have two-source information (i.e., graph structure and node attributes) to sufficiently negotiate with each other for accurate data imputation. By this means, more discriminative latent features could be adaptively collected and preserved to perform high-quality attribute restoration.
- Through experimental results on four benchmarks, we have demonstrated that ITR significantly and consistently outperforms the state-of-the-art counterparts on both profiling and node classification tasks.

2 Related Work

Graph Representation Learning. Early solutions to graph representation learning (GRL) mainly include random walk-based methods [Perozzi *et al.*, 2014; Grover and Leskovec, 2016], which first generate the random walk sequences over the network structure properties and then utilize a Skip-Gram model to learn graph representations. These methods heavily rely on structure information and overlook other available properties in the graph, such as attribute information. More recently, since the powerful neighborhood aggregation capacity of graph neural networks (GNNs), many efforts have been made to design GNN-based representation learning methods. These methods can be approximately divided into generative/predictive learning-based methods [Kipf and Welling, 2016; Tu *et al.*, 2021; Liu *et al.*, 2022] and contrastive learning-based methods [Hassani and Ahmadi, 2020; Peng *et al.*, 2020; Zhu *et al.*, 2021]. One underlying assumption commonly adopted by these methods is that the attributes of all nodes are complete. While in real-world scenarios, they may suffer significant performance degradation when handling incomplete graphs.

Data Imputation for Incomplete Graphs. To handle incomplete graphs, data imputation has been widely integrated with machine learning techniques, such as matrix completion,

generative adversarial network, and Gaussian mixture model (GMM). For example, NMTR [Gao *et al.*, 2019] and GRAPE [You *et al.*, 2020], the popular matrix completion methods, first regard the user-item rating matrix, users (or items), and the observed ratings as a bipartite graph, node attributes, and linkage relations, respectively. Then these methods employ a GNN-based framework to estimate the probabilities (viewed as imputed values) of absent linkage relations. More recently, GINN [Spinelli *et al.*, 2020] first initializes the incomplete values by a binary mask matrix before network training, and then learns a graph adversarially-trained framework to perform attribute restoration. GCNMF [Taguchi *et al.*, 2021] employs GMM to estimate the incomplete information based on the available one, and in the meanwhile, jointly optimizes GMM and GNN in a united framework. Despite their significant progress, these methods 1) are not suitable for attribute-missing scenarios, or 2) disconnect the processes of data imputation and algorithm optimization. To address these issues, an advanced method called SAT [Chen *et al.*, 2022] puts forward to unify data imputation and network learning processes into a single optimization procedure, where two-source information embeddings are learned in a decoupled scheme and then aligned with the Gaussian noise for data imputation. However, to complete the missing values, SAT isolates the learning processes of two-source information embeddings and imposes too strict a distribution assumption on the latent variables, resulting in inaccurate imputation.

3 The Proposed Method

3.1 Notations

Given an undirected graph $\mathcal{G} = \{\mathcal{V}, \mathcal{E}\}$ with C classes, where $\mathcal{V} = \{\mathbf{v}_1, \mathbf{v}_2, \dots, \mathbf{v}_N\}$, \mathcal{E} , and N are the node set, edge set, and the number of nodes, respectively. In classic graph learning, a graph is usually characterized by its attribute matrix $\mathbf{X} \in \mathbb{R}^{N \times D}$ and normalized adjacency matrix $\tilde{\mathbf{A}} \in \mathbb{R}^{N \times N}$, where D is the node attribute dimension [Kipf and Welling, 2017]. Specially, in the attribute-missing case, with the existence of missing values, we further define $\mathcal{V}^o = \{\mathbf{v}_1^o, \mathbf{v}_2^o, \dots, \mathbf{v}_{N^o}^o\}$ and $\mathcal{V}^m = \{\mathbf{v}_1^m, \mathbf{v}_2^m, \dots, \mathbf{v}_{N^m}^m\}$ to be the set of attribute-observed samples and the set of attribute-missing samples, respectively. Accordingly, $\mathcal{V} = \mathcal{V}^o \cup \mathcal{V}^m$, $\mathcal{V}^o \cap \mathcal{V}^m = \emptyset$, and $N = N^o + N^m$.

3.2 Two-source Information Extraction

Unlike most current imputation-based GRL methods that perform data imputation before network training, our goal is to make full use of all trustworthy observations, i.e., attribute-observed sample information and graph structure information, to accurately impute and restore the unknown features by unifying imputation and network learning into a single optimization procedure. To this end, as shown in Fig. 1, we introduce a pseudo-Siamese architecture, which employs two identical 2-layer graph convolution networks (GCNs) as graph encoders, denoted as $E_a(\cdot)$ and $E_s(\cdot)$, respectively. Here we take $E_a(\cdot)$ as an example to introduce the learning process of attribute-observed sample embeddings, and the learning procedure of $E_s(\cdot)$ is similar. Specifically, the encoder $E_a(\cdot)$ initially accepts a given observed sub-graph

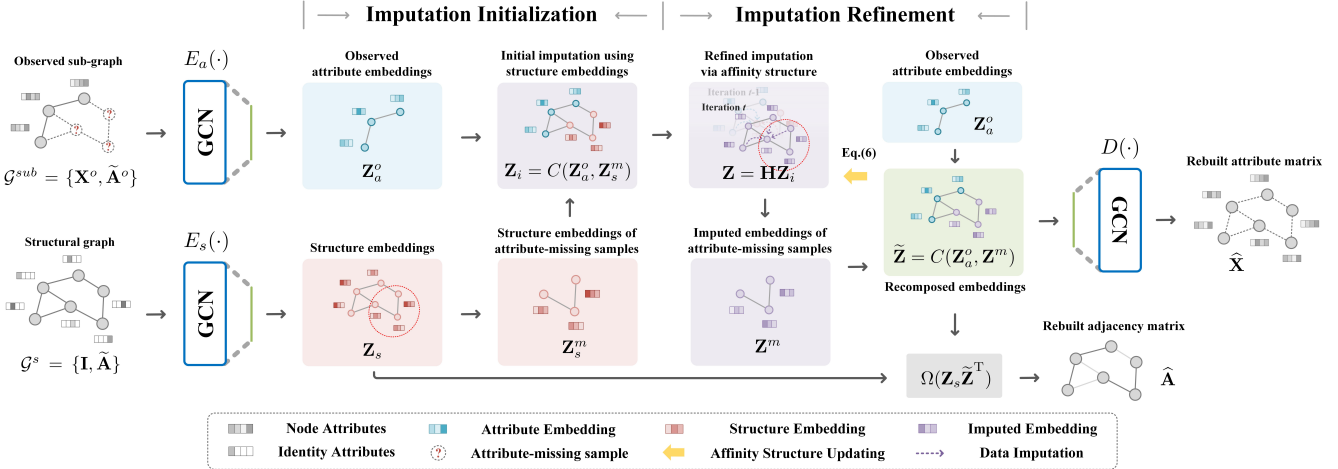


Figure 1: Overall framework of Initializing Then Refining (ITR). To impute the missing values, we first adopt the structure embeddings of the attribute-missing samples as the embedding initialization, and then adaptively refine these initial values by aggregating the reliable and informative information of the attribute-observed samples according to the affinity structure.

$\mathcal{G}^{sub} = \{\mathbf{X}^o, \tilde{\mathbf{A}}^o\}$ as input, where $\mathbf{X}^o \in \mathbb{R}^{N^o \times D}$ and $\tilde{\mathbf{A}}^o \in \mathbb{R}^{N^o \times N^o}$ denote the observed attribute matrix and the corresponding normalized adjacency matrix. Then we compute l -th latent representations of attribute-observed samples $\mathbf{Z}_a^{(l)}$:

$$\mathbf{Z}_a^{(l)} = \sigma(\tilde{\mathbf{A}}^o \mathbf{Z}_a^{(l-1)} \mathbf{W}^{(l)}), \quad (1)$$

where $\mathbf{W}^{(l)}$ indicates the encoder network parameters of the l -th layer. $\sigma(\cdot)$ denotes the ReLU activation function. Similarly, the encoder $E_s(\cdot)$ receives a given structural graph $\mathcal{G}^s = \{\mathbf{I}, \tilde{\mathbf{A}}\}$ and outputs $\mathbf{Z}_s^{(l)}$, where $\mathbf{I} \in \mathbb{R}^{N \times N}$ is identity matrix and $\mathbf{Z}_s^{(l)}$ denotes l -th latent representations of \mathcal{G}^s .

3.3 Initializing Then Refining

Imputation Initialization. Since only partial samples with complete attributes exist, assigning initial values to the attribute-missing ones should be considered before network training. A commonly adopted way is classic data imputation, e.g., zero-filling and mean value-filling. However, in the attribute-missing case, these tricks may introduce much irrelevant information that readily diffuses through the network, resulting in semantically biased representations. To avoid this issue, an underlying solution is to leverage the graph structure information of attribute-missing samples to implement the initial imputation in the latent space. Since the structural properties of the entire graph data are complete, the initialization for attribute-missing samples is reliable. Specifically, after obtaining two-source embeddings, i.e., $\mathbf{Z}_a \in \mathbb{R}^{N^o \times d}$ and $\mathbf{Z}_s \in \mathbb{R}^{N \times d}$, we first select the structure embeddings of attribute-missing samples $\mathbf{Z}_s^m \in \mathbb{R}^{N^m \times d}$ from \mathbf{Z}_s , and then combine them with observed attribute embeddings \mathbf{Z}_a^o using Concat function $C(\cdot)$. As illustrated in Fig. 1, the concatenation operation to construct \mathbf{Z}_i is not the classic channel concatenation. In this operation, we fill the embeddings of attribute-observed samples with \mathbf{Z}_a^o and the embeddings of attribute-missing samples with \mathbf{Z}_s^m :

$$\mathbf{Z}_i = C(\mathbf{Z}_a^o, \mathbf{Z}_s^m), \quad (2)$$

Dataset	Method	Recall@50	NDCG@50
Cora	Ours-Z	34.03	32.08
	Ours-S	<u>34.77</u>	<u>32.95</u>
	Ours-S-A	36.47 (1.70↑)	34.60 (1.65↑)
Citeseer	Ours-Z	24.04	25.32
	Ours-S	<u>24.91</u>	<u>26.55</u>
	Ours-S-A	26.84 (1.93↑)	28.69 (2.14↑)

Table 1: Performance comparison. The boldface and underline values indicate the best and the sub-optimal results, respectively. \uparrow denotes the performance improvement of Ours-S-A against Ours-S.

where we denote the initially imputed embeddings as $\mathbf{Z}_i \in \mathbb{R}^{N \times d}$. d is the embedding dimension. Please note that the position of each sample is kept unchanged within the graph.

Imputation Refinement. As known, the attributes preserve the graph semantics while the structures describe the linkage relations among nodes. Hence, the discriminative capacities of both types of information exhibit differences to some extent. To verify whether our assumption holds, we compare three methods and present analyses on Cora and Citeseer. Ours-Z, Ours-S, and Ours-S-A are methods where we impute the attribute-missing part in the latent space with zero values, the structure embeddings merely, and the structure-attribute embeddings, respectively. From the results in Table 1, we observe that the Ours-S method consistently outperforms the Ours-Z method but is not comparable to the Ours-S-A method. These results hold our expectation and clearly illustrate that although the structure embeddings could effectively serve the initial imputation task, there still exists noise in \mathbf{Z}_s^m that would affect the discriminative capacity of latent representations, thus leading to sub-optimal performance. To address this limitation, we try to refine the imputation process by transferring the available semantics \mathbf{Z}_a^o into \mathbf{Z}_s^m via an affinity structure $\mathbf{H} \in \mathbb{R}^{N \times N}$. The intuition behind this is that the sample embeddings \mathbf{Z}_a^o are reliable since the attribute information of all attribute-observed samples is complete. In this way, the semantic gap between \mathbf{Z}_a^o and \mathbf{Z}_s^m could be narrowed to boost the expressive capacity of the whole embed-

dings. The above learning process can be formulated as below (i.e., a graph convolution-like operation):

$$\mathbf{Z} = \mathbf{H}\mathbf{Z}_i, \quad (3)$$

where we denote the imputed embeddings as $\mathbf{Z} \in \mathbb{R}^{N \times d}$, here we set the affinity structure \mathbf{H} to $\tilde{\mathbf{A}}$ for initialization.

In Eq.(3), we observe that the noise information in \mathbf{Z}_s^m can also diffuse across the attribute-observed part, which would make the representations of \mathbf{Z}_a^o less discriminative. In this circumstance, conducting the embeddings of both attribute-observed and attribute-missing samples simultaneously would undermine the quality of sample embeddings and the reconstruction accuracy of available samples, which would in turn affect the subsequent data imputation tasks and even distort the original graph. To overcome this issue, we introduce an information recomposing scheme. Firstly, we merely select the latent variables of attribute-missing samples $\mathbf{Z}^m \in \mathbb{R}^{N^m \times d}$ from \mathbf{Z} , and then recompose them with \mathbf{Z}_a^o :

$$\tilde{\mathbf{Z}} = C(\mathbf{Z}_a^o, \mathbf{Z}^m), \quad (4)$$

where we denote the recomposed embeddings as $\tilde{\mathbf{Z}} \in \mathbb{R}^{N \times d}$. In our settings, the information recomposing operation replaces the adjusted embeddings of attribute-observed samples with more reliable \mathbf{Z}_a^o . By doing this, we reduce the adverse effect of inaccurate information passing from the embeddings of attribute-missing samples. Moreover, the embeddings of attribute-observed samples are fixed as \mathbf{Z}_a^o in the final step, as shown in Fig. 1. This provides the most trustworthy information of those samples for subsequent data imputation tasks.

It is worth noting that the initial affinity matrix \mathbf{H} (i.e., $\tilde{\mathbf{A}}$) is not the ground truth. The errors within this matrix are two-fold: 1) noisy connections. Besides inner connections within clusters, inappropriate connections could exist between clusters in the matrix; 2) missing connections. In $\tilde{\mathbf{A}}$, only the first-order connections are recorded, the higher-order connections could be missing. Both would cause the inaccurate reconstruction of observed attributes and missing attributes. To overcome these issues, we seek to refine \mathbf{H} to further improve the imputation quality via an affinity structure updating scheme. Specifically, we first generate a normalized self-correlated matrix $\mathbf{S} \in \mathbb{R}^{N \times N}$ according to $\tilde{\mathbf{Z}}$ as below:

$$\mathbf{S}_{jk} = \mathcal{N}\left(\frac{\tilde{\mathbf{z}}_j \tilde{\mathbf{z}}_k^T}{\|\tilde{\mathbf{z}}_j\| \|\tilde{\mathbf{z}}_k\|}\right), \quad \forall j, k \in [1, N], \quad (5)$$

where $\mathcal{N}(\mathbf{Y}) = \mathbf{D}_Y^{-\frac{1}{2}} \mathbf{Y} \mathbf{D}_Y^{-\frac{1}{2}}$ denotes the structural normalization function, $\mathbf{D}_Y \in \mathbb{R}^{N \times N}$ is the degree matrix of \mathbf{Y} . $\tilde{\mathbf{z}}_j$ ($\tilde{\mathbf{z}}_k$) indicates the embedding of node v_j (v_k). Then we update the affinity structure \mathbf{H} every t iterations via Eq.(6), and adopt it to refine the subsequent imputation process:

$$\mathbf{H} = \alpha \tilde{\mathbf{A}} + (1 - \alpha) \mathbf{S}, \quad (6)$$

where α is a balanced coefficient, and we initialize it as 0.5. In this way, the affinity structure updating operation allows the network to construct the embeddings of attribute-missing samples with not only the first-order but also the higher-order connections from the original graph. Since the embeddings of attribute-observed samples become more reliable and the embeddings of attribute-missing samples become more informative, the quality of the overall graph embeddings is boosted.

Dataset	Nodes	Edges	Dimension	Classes
Cora	2708	5278	1433	7
Citeseer	3327	4228	3703	6
Amac	13752	245861	767	10
Amap	7650	119081	745	8

Table 2: Summary of datasets.

3.4 Decoding and Model Training

Finally, we directly feed $\tilde{\mathbf{Z}}$ with $\tilde{\mathbf{A}}$ into the decoder $D(\cdot)$ to complete the attribute restoration, which is formulated as:

$$\tilde{\mathbf{Z}}^{(l)} = \sigma(\tilde{\mathbf{A}} \tilde{\mathbf{Z}}^{(l-1)} \widetilde{\mathbf{W}}^{(l)}), \quad (7)$$

where $\widetilde{\mathbf{W}}^{(l)}$ indicates the decoder network parameters of the l -th layer. $\tilde{\mathbf{Z}}^{(0)}$ and $\tilde{\mathbf{Z}}^{(2)}$ denote the recomposed embeddings $\tilde{\mathbf{Z}}$ and the rebuilt attribute matrix $\widehat{\mathbf{X}} \in \mathbb{R}^{N \times D}$, respectively.

The overall objective of ITR consists of two parts:

$$\mathcal{L}_a = \frac{1}{2N^o} \|\mathbf{X}^o - \widehat{\mathbf{X}}^o\|_F^2, \quad (8)$$

$$\mathcal{L}_s = \frac{1}{N^2} \sum_{i=1}^N \sum_{j=1}^N BCE(\tilde{\mathbf{A}}_{ij}, \widehat{\mathbf{A}}_{ij}), \quad (9)$$

$$\mathcal{L} = \gamma \mathcal{L}_a + \lambda \mathcal{L}_s. \quad (10)$$

In Eq.(10), \mathcal{L}_a refers to the mean square error (MSE) between the attribute-observed part of both \mathbf{X} and $\widehat{\mathbf{X}}$. \mathcal{L}_s refers to the binary cross-entropy (BCE) between the normalized adjacency matrix $\tilde{\mathbf{A}}$ and the rebuilt adjacency matrix $\widehat{\mathbf{A}} \in \mathbb{R}^{N \times N}$, where $\widehat{\mathbf{A}} = \Omega(\mathbf{Z}_s \tilde{\mathbf{Z}}^T)$, $\Omega(\cdot)$ is a sigmoid activation function. λ and γ are two balanced coefficients.

4 Experiments

4.1 Experimental Setup

Benchmark Datasets. We conduct experiments to evaluate the proposed ITR on four benchmark datasets, including Cora [McCallum *et al.*, 2000], Citeseer [Sen *et al.*, 2008], Amazon Computer (Amac), and Amazon Photo (Amap) [Shchur *et al.*, 2018]. Table 2 summarizes the dataset information.

Parameters Setting. For all compared methods except for GINN [Spinelli *et al.*, 2020] and GCNMF [Taguchi *et al.*, 2021], the experimental results are acquired according to the paper of SAT [Chen *et al.*, 2022]. For GINN and GCNMF methods, we run their public code by following the settings of the original papers, and then report the corresponding performance. For our proposed ITR, we strictly follow the principle of data splits as was done in SAT [Chen *et al.*, 2022], including the split ratio of attribute-observed/-missing samples and the split ratio of train/test sets. Specifically, 1) in the profiling task, we randomly sample 40% nodes with attributes as the training set, and manually mask all attributes of the rest of 10% and 50% nodes (i.e., attribute-missing samples) as the validation set and the test set, respectively. We employ a symmetric backbone framework consisting of 4-layer GCNs and optimize it with the Adam optimization algorithm, where we set the learning rate to 1e-3. During the training phase, we transfer all samples into our ITR to restore missing attributes

Dataset	Metric	NeighAggre	VAE	GCN	GraphSage	GAT	Hers	GraphRNA	ARWMF	SAT	Ours
Cora	Recall@10	0.0906	0.0887	0.1271	0.1284	0.1350	0.1226	0.1395	0.1291	<u>0.1508</u>	0.1682
	Recall@20	0.1413	0.1228	0.1772	0.1784	0.1812	0.1723	0.2043	0.1813	<u>0.2182</u>	0.2369
	Recall@50	0.1961	0.2116	0.2962	0.2972	0.2972	0.2799	0.3142	0.2960	<u>0.3429</u>	0.3647
	NDCG@10	0.1217	0.1224	0.1736	0.1768	0.1791	0.1694	0.1934	0.1824	<u>0.2112</u>	0.2320
	NDCG@20	0.1548	0.1452	0.2076	0.2102	0.2099	0.2031	0.2362	0.2182	<u>0.2546</u>	0.2781
	NDCG@50	0.1850	0.1924	0.2702	0.2728	0.2711	0.2596	0.2938	0.2776	<u>0.3212</u>	0.3460
Citeseer	Recall@10	0.0511	0.0382	0.0620	0.0612	0.0561	0.0576	<u>0.0777</u>	0.0552	0.0764	0.0963
	Recall@20	0.0908	0.0668	0.1097	0.1097	0.1012	0.1025	0.1272	0.1015	<u>0.1280</u>	0.1548
	Recall@50	0.1501	0.1296	0.2052	0.2058	0.1957	0.1973	0.2271	0.1952	<u>0.2377</u>	0.2684
	NDCG@10	0.0823	0.0601	0.1026	0.1003	0.0878	0.0904	0.1291	0.0859	<u>0.1298</u>	0.1632
	NDCG@20	0.1155	0.0839	0.1423	0.1393	0.1253	0.1279	0.1703	0.1245	<u>0.1729</u>	0.2120
	NDCG@50	0.1560	0.1251	0.2049	0.2034	0.1872	0.1900	0.2358	0.1858	<u>0.2447</u>	0.2869
Amac	Recall@10	0.0321	0.0255	0.0273	0.0269	0.0271	0.0273	0.0386	0.0280	0.0391	0.0448
	Recall@20	0.0593	0.0502	0.0533	0.0528	0.0530	0.0525	0.0690	0.0544	<u>0.0703</u>	0.0781
	Recall@50	0.1306	0.1196	0.1275	0.1278	0.1278	0.1273	0.1465	0.1289	<u>0.1514</u>	0.1620
	NDCG@10	0.0788	0.0632	0.0671	0.0664	0.0673	0.0676	0.0931	0.0694	<u>0.0963</u>	0.1095
	NDCG@20	0.1156	0.0970	0.1027	0.1020	0.1028	0.1025	0.1333	0.1053	<u>0.1379</u>	0.1537
	NDCG@50	0.1923	0.1721	0.1824	0.1822	0.1830	0.1825	0.2155	0.1851	<u>0.2243</u>	0.2429
Amap	Recall@10	0.0329	0.0276	0.0294	0.0295	0.0294	0.0292	0.0390	0.0294	0.0410	0.0436
	Recall@20	0.0616	0.0538	0.0573	0.0562	0.0573	0.0574	0.0703	0.0568	<u>0.0743</u>	0.0782
	Recall@50	0.1361	0.1279	0.1324	0.1322	0.1324	0.1328	0.1508	0.1327	<u>0.1597</u>	0.1643
	NDCG@10	0.0813	0.0675	0.0705	0.0712	0.0705	0.0714	0.0959	0.0727	<u>0.1006</u>	0.1073
	NDCG@20	0.1196	0.1031	0.1082	0.1079	0.1083	0.1094	0.1377	0.1098	<u>0.1450</u>	0.1533
	NDCG@50	0.1998	0.1830	0.1893	0.1896	0.1892	0.1906	0.2232	0.1915	<u>0.2359</u>	0.2450

Table 3: Profiling performance comparison. The boldface and underline values indicate the best and the sub-optimal results, respectively.

Type	Dataset	NeighAggre	VAE	GCN	GraphSage	GAT	Hers	GraphRNA	ARWMF	GINN	GCNMF	SAT	Ours
X	Cora	0.6248	0.2826	0.3943	0.4852	0.4143	0.3046	0.7581	<u>0.7769</u>	-	-	0.7644	0.8143
	Citeseer	0.5593	0.2551	0.3768	0.3933	0.2129	0.2585	<u>0.6320</u>	0.2267	-	-	0.6010	0.6715
	Amac	<u>0.8365</u>	0.3747	0.3660	0.3747	0.3747	0.3747	0.6968	0.5608	-	-	0.7410	0.8388
	Amap	<u>0.8846</u>	0.2598	0.2683	0.2598	0.2598	0.2598	0.8407	0.4675	-	-	0.8762	0.9075
X+A	Cora	0.6494	0.3011	0.4387	0.5779	0.4525	0.3405	0.8198	0.8025	0.6758	0.7030	<u>0.8327</u>	0.8556
	Citeseer	0.5413	0.2663	0.4079	0.4278	0.2688	0.3229	0.6394	0.2764	0.5532	0.6340	<u>0.6599</u>	0.6809
	Amac	<u>0.8715</u>	0.4023	0.3974	0.4019	0.4034	0.4025	0.8650	0.7400	0.8127	0.7643	<u>0.8519</u>	0.8765
	Amap	0.9010	0.3781	0.3656	0.3784	0.3789	0.3794	0.9207	0.6146	0.8777	0.8779	0.9163	<u>0.9187</u>

Table 4: Node classification performance comparison. The boldface and underline indicate the best and the sub-optimal results, respectively.

by merely reconstructing the attribute-observed samples (i.e., training set). After training, we directly generate the rebuilt attribute matrix over the well-trained model via forwarding propagation; 2) in the node classification task, the restored attributes are randomly split into 80% and 20% for training and testing. We train the classifier with five-fold validation for 1000 iterations and repeat the experiments 10 times. Moreover, the learning rate, the latent dimension, the dropout rate, and the weight decay are set to 1e-3, 64, 0.5, and 5e-4, respectively. Please note that we do not carefully tune these parameters for the ease of training as was done in SAT.

4.2 Performance Comparison

In the profiling task, for fairness, we follow the baseline settings of SAT and compare ITR with nine methods using Recall and NDCG as metrics, including a classical profiling method **NeighAggre** [Özgür Simsek and Jensen, 2008]; an auto-encoder-based method **VAE** [Kingma and Welling, 2014]; three typical GCN-based methods, i.e., **GCN** [Kipf and Welling, 2017], **GraphSage** [Hamilton *et al.*, 2017], and **GAT** [Velickovic *et al.*, 2018]; two attributed random walk-based methods, i.e., **GraphRNA** [Huang *et al.*, 2019] and **ARWMF** [Chen *et al.*, 2019]; a cold-start recommendation method **Hers** [Hu *et al.*, 2019]; an attribute-missing GRL method **SAT** [Chen *et al.*, 2022]. In addition, we compare ITR with two attribute-incomplete GRL methods, i.e., **GINN** [Spinelli *et al.*, 2020], **GCNMF** [Taguchi *et al.*, 2021], and report their accuracy performance for node classification.

As shown in Table 3, we can see that ITR outperforms all compared methods in terms of six metrics on four datasets. Taking the results of Recall@50 and NDCG@50 for example, SAT has been considered the strongest attribute-missing GRL method. The proposed ITR exceeds it by 2.18%/2.48%, 3.07%/4.22%, 1.06%/1.86%, and 0.46%/0.91% on four datasets, respectively. Moreover, Table 4 illustrates the node classification performance of all compared methods. “X” or “X+A” indicates that we perform the node classification task to estimate the quality of the attribute restoration using merely attribute or both structure-attribute information. From the results on four datasets, we observe that 1) the recently proposed attribute-incomplete GRL methods (i.e., GINN and GCNMF) are not comparable to ours, ITR exceeds them by at least 15.26%, 4.69%, 6.38%, and 4.08% accuracy increment; 2) ITR gains 4.99%, 7.05%, 9.78%, and 3.13% performance enhancement over the state-of-the-art method SAT. The above results on two tasks have solidly verified the effectiveness of ITR. These benefits can be attributed to the following merits: 1) different from the compared methods, for handling attribute-missing graphs, we develop a more expressive imputation network that avoids the reliance on any prior distribution assumption; 2) ITR can make full use of the trustworthy visible information to conduct the sample embeddings for high-quality attribute restoration; 3) we introduce a more general and flexible imputation strategy, which can facilitate the negotiation between attribute and structure information for accurate data imputation.

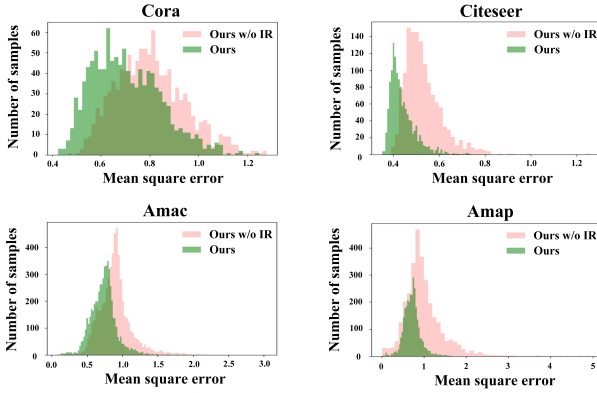


Figure 2: Effect of the information recomposing (IR) and affinity structure updating (ASU) schemes for node classification.

Dataset	Metric	Ratio	SAT	Ours
Cora	Recall@10	20%	0.1349	0.1421
		40%	0.1471	0.1682
		60%	0.1559	0.1775
		80%	0.1743	0.1841
	NDCG@10	20%	0.1933	0.1998
		40%	0.2060	0.2320
		60%	0.2179	0.2433
		80%	0.2401	0.2560
Citeseer	Recall@10	20%	0.0630	0.0740
		40%	0.0778	0.0963
		60%	0.0832	0.1061
		80%	0.0837	0.1100
	NDCG@10	20%	0.1063	0.1264
		40%	0.1341	0.1632
		60%	0.1435	0.1779
		80%	0.1441	0.1857

Table 5: Profiling performance comparison of SAT and our ITR with different observed ratios on Cora and Citeseer. The boldface values indicate the best results.

4.3 Ablation Study

Effect of Each Component. To verify the benefit of each component, we conduct ablation studies on four datasets for ITR and two ITR variants, each of which has one of the key components removed. ITR w/o IR and ITR w/o ASU indicate the method with information recomposing and affinity structure updating being masked, respectively. From the results in Fig. 2, we observe that the accuracy of ITR on the four datasets would degrade without one of the key components. Specifically, for the “X” task, ITR exceeds ITR w/o IR by 2.54%, 1.53%, 2.24%, and 1.64% accuracy increment, and ITR w/o ASU by 0.69%, 0.30%, 0.98%, and 0.55% accuracy increment on Cora, Citeseer, Amac, and Amap, respectively. We find that the information recomposing scheme plays a more important role than the information refining scheme. To visually illustrate this point, we present the mean square error (MSE) comparison of ITR and ITR w/o IR at the last training iteration. As seen in Fig. 3, it is obvious that, with the information recomposing scheme, the method can achieve a good convergence as well as a high-quality attribute restoration.

Analysis of the Observed Ratio. To further show the superiority of ITR, we compare it with the strongest baseline SAT on Cora and Citeseer by varying the observed ratio from 20% to 80%. As shown in Table 5, taking the results of Recall@10

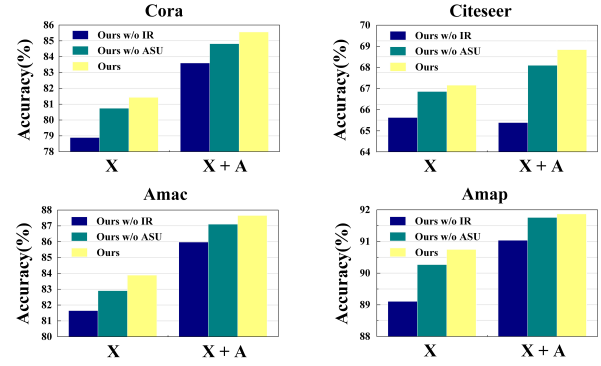


Figure 3: MSE comparison of ITR and an ITR variant. Ours w/o IR denotes the ITR without information recomposing scheme.

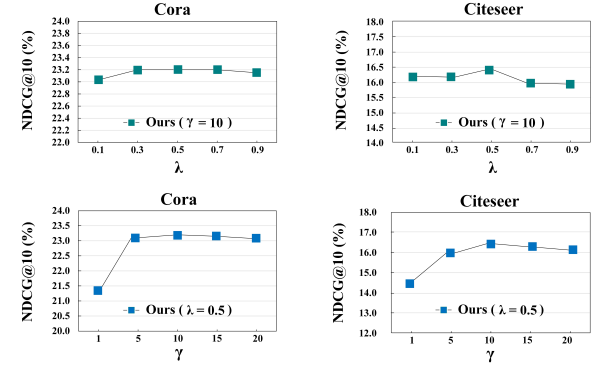


Figure 4: Hyper-parameters analysis on Cora and Citeseer.

on Citeseer for example, our ITR outperforms SAT by 1.10%, 1.85%, 2.29%, and 2.63% with the variation of observed ratio from 20% to 80%. The improvement is more significant with the increase in the observed ratio. This observation has well verified the robustness of our ITR.

Hyper-parameter Analysis. Fig. 4 reports the NDCG@10 performance variation of ITR on Cora and Citeseer when λ and γ vary from 0.1 to 0.9 and 1 to 20, respectively. From the figures, we observe that 1) for a specific γ value, the performance shows a trend of first rising and then dropping slightly with the variation of λ . This indicates that our ITR needs a proper coefficient for auxiliary loss to rebuild the adjacency matrix. The observations of γ are similar; 2) ITR tends to perform well by setting λ and γ to 0.5 and 10, respectively.

5 Conclusion

In this work, we have designed a novel graph attribute imputation approach called ITR toward attribute-missing graph representation learning. In our method, an initializing then refining strategy is carefully designed to perform data imputation in an adaptive manner. By this means, two-source information is allowed to sufficiently negotiate with each other in the latent space. Thus the expressive capacity of imputed variables can be improved for high-quality attribute restoration. Extensive experimental results have verified the superiority and effectiveness of our proposed ITR.

Acknowledgments

This work is supported by the National Key R&D Program of China (Grant No. 2018YFB1800202, 2020YFC2003400, and 2020AAA0107100), the National Natural Science Foundation of China (Grant No. 61922088, 62006237, 62072465, 62162024, and 62162022).

References

- [Chen *et al.*, 2019] Lei Chen, Shunwang Gong, Joan Bruna, and Michael M. Bronstein. Attributed random walk as matrix factorization. In *NeurIPS Workshop*, 2019.
- [Chen *et al.*, 2022] Xu Chen, Siheng Chen, Jiangchao Yao, Huangjie Zheng, Ya Zhang, and Ivor W. Tsang. Learning on attribute-missing graphs. *IEEE TPAMI*, 44(2):740–757, 2022.
- [Gao *et al.*, 2019] Chen Gao, Xiangnan He, Dahua Gan, Xiangning Chen, Fuli Feng, Yong Li, TatSeng Chua, and De-peng Jin. Neural multi-task recommendation from multi-behavior data. In *ICDE*, page 1554–1557, 2019.
- [Grover and Leskovec, 2016] Aditya Grover and Jure Leskovec. node2vec: Scalable feature learning for networks. In *KDD*, pages 855–864, 2016.
- [Hamilton *et al.*, 2017] William L. Hamilton, Zhitao Ying, and Jure Leskovec. Inductive representation learning on large graphs. In *NeurIPS*, pages 1024–1034, 2017.
- [Hassani and Ahmadi, 2020] Kaveh Hassani and Amir Hossein Khas Ahmadi. Contrastive multi-view representation learning on graphs. In *ICML*, pages 4116–4126, 2020.
- [Hu *et al.*, 2017] Pengwei Hu, Keith C. C. Chan, and Tiantian He. Deep graph clustering in social network. In *WWW*, pages 1425–1426, 2017.
- [Hu *et al.*, 2019] Liang Hu, Songlei Jian, Longbing Cao, Zhiping Gu, Qingkui Chen, and Artak Amirkbeikyan. Hers: Modeling influential contexts with heterogeneous relations for sparse and cold-start recommendation. In *AAAI*, pages 3830–3837, 2019.
- [Huang *et al.*, 2019] Xiao Huang, Qingquan Song, Yuening Li, and Xia Hu. Graph recurrent networks with attributed random walks. In *KDD*, pages 732–740, 2019.
- [Kingma and Welling, 2014] Diederik P. Kingma and Max Welling. Auto-encoding variational bayes. In *ICLR*, 2014.
- [Kipf and Welling, 2016] Thomas N. Kipf and Max Welling. Variational graph auto-encoders. In *ArXiv abs/1611.07308*, 2016.
- [Kipf and Welling, 2017] Thomas N. Kipf and Max Welling. Semi-supervised classification with graph convolutional networks. In *ICLR*, 2017.
- [Liu *et al.*, 2022] Yue Liu, Wenxuan Tu, Sihang Zhou, Xinwang Liu, Linxuan Song, Xihong Yang, and En Zhu. Deep graph clustering via dual correlation reduction. In *AAAI*, 2022.
- [McCallum *et al.*, 2000] Andrew McCallum, Kamal Nigam, Jason Rennie, and Kristie Seymore. Automating the construction of internet portals with machine learning. *Information Retrieval*, 3(2):127–163, 2000.
- [Peng *et al.*, 2020] Zhen Peng, Wenbing Huang, Minnan Luo, Qinghua Zheng, Yu Rong, Tingyang Xu, and Junzhou Huang. Graph representation learning via graphical mutual information maximization. In *WWW*, pages 259–270, 2020.
- [Perozzi *et al.*, 2014] Bryan Perozzi, Rami Al-Rfou, and Steven Skiena. Deepwalk: online learning of social representations. In *KDD*, pages 701–710, 2014.
- [Sen *et al.*, 2008] Prithviraj Sen, Galileo Namata, Mustafa Bilgic, Lise Getoor, Brian Gallagher, and Tina Eliassi-Rad. Collective classification in network data. *Information Retrieval*, 29(3):93–106, 2008.
- [Shchur *et al.*, 2018] Oleksandr Shchur, Maximilian Mumme, Aleksandar Bojchevski, and Stephan Günnemann. Pitfalls of graph neural network evaluation. In *ArXiv abs/1811.05868*, 2018.
- [Spinelli *et al.*, 2020] Indro Spinelli, Simone Scardapane, and Aurelio Uncini. Missing data imputation with adversarially-trained graph convolutional networks. *Neural Networks*, 129:249–260, 2020.
- [Taguchi *et al.*, 2021] Hibiki Taguchi, Xin Liu, and Tsuyoshi Murata. Graph convolutional networks for graphs containing missing features. *Future Generation Computer Systems*, 117:155–168, 2021.
- [Tu *et al.*, 2021] Wenxuan Tu, Sihang Zhou, Xinwang Liu, Xifeng Guo, Zhiping Cai, En Zhu, and Jieren Cheng. Deep fusion clustering network. In *AAAI*, pages 9978–9987, 2021.
- [van den Berg *et al.*, 2017] Rianne van den Berg, Thomas N Kipf, and Max Welling. Graph convolutional matrix completion. In *ArXiv abs/1706.02263*, 2017.
- [Velickovic *et al.*, 2018] Petar Velickovic, Guillem Cucurull, Arantxa Casanova, Adriana Romero, Pietro Liò, and Yoshua Bengio. Graph attention networks. In *ICLR*, 2018.
- [Wu *et al.*, 2020] Jiapeng Wu, Meng Cao, Jackie Chi Kit Cheung, and William L. Hamilton. Temp: Temporal message passing for temporal knowledge graph completion. In *EMNLP*, pages 5730–5746, 2020.
- [You *et al.*, 2020] Jiaxuan You, Xiaobai Ma, Daisy Yi Ding, Mykel J. Kochenderfer, and Jure Leskovec. Handling missing data with graph representation learning. In *NeurIPS*, 2020.
- [Zhang and Chen, 2020] Muhan Zhang and Yixin Chen. Inductive matrix completion based on graph neural networks. In *ICLR*, 2020.
- [Zhu *et al.*, 2021] Yanqiao Zhu, Yichen Xu, Feng Yu, Qiang Liu, Shu Wu, and Liang Wang. Graph contrastive learning with adaptive augmentation. In *WWW*, pages 2069–2080, 2021.
- [Özgür Simsek and Jensen, 2008] Özgür Simsek and David D. Jensen. Navigating networks by using homophily and degree. *National Academy of Sciences*, 105(35):12758–12762, 2008.